THE AMERICAN SOCIETY OF MECHANICAL ENGINEERS
345 E. 47th St., New York, N.Y. 10017

96-GT-223

COMPARISON OF PREDICTED AND EXPERIMENTAL NUSSELT NUMBER FOR A FILM-COOLED ROTATING BLADE

Vijay K. Garg
AYT Corporation
c/o NASA Lewis Research Center
Cleveland, OH 44135

Reza S. Abhari
Dept. of Aerospace Eng., Applied Mechanics & Aviation
The Ohio State University
Columbus, OH 43210

BREAK

ABSTRACT

The predictions from a three-dimensional Navier-Stokes code have been compared to the Nusselt number data obtained on a film-cooled, rotating turbine blade. The blade chosen is the ACE rotor with five rows containing 93 film cooling holes covering the entire span. This is the only film-cooled rotating blade over which experimental heat transfer data is available for the present comparison. Over 2.25 million grid points are used to compute the flow over the blade. Usually in a film cooling computation on a stationary blade, the computational domain is just one spanwise pitch of the film-cooling holes, with periodic boundary conditions in the span direction. However, for a rotating blade, the computational domain consists of the entire blade span from hub to tip, as well as the tip clearance region.

As far as the authors are aware of, the present work offers the first comparison of the prediction of surface heat transfer using a three dimensional CFD code with film injection and the measured heat flux on a fully film-cooled rotating transonic turbine blade. In a detailed comparison with the measured data on the suction surface, a reasonably good comparison is obtained, particularly near the hub section. On the pressure surface, however, the comparison between the data and the prediction is poor. A potential reason for the discrepancy on the pressure surface could be the presence of unsteady effects due to stator-rotor interaction in the experiments which are not modeled in the present numerical computations.

NOMENCLATURE

B_p blowing parameter [$= (\rho_c V_c)/\{\rho_o(RT_o)^{1/2}\}$]
c_a axial chord of the blade
C_D discharge coefficient for the hole
d coolant hole diameter
k thermal conductivity
Nu Nusselt number based on c_a, $(T_{o,rel} - T_w)$ and k_w
p pressure
r radial coordinate
R gas constant
s distance from the leading edge along the pressure or suction surface
S $= s/s_m$ on suction surface, and $= - s/s_m$ on pressure surface
T temperature
V_c average coolant velocity at the hole exit
y y-coordinate of the Cartesian coordinate system with origin at the geometric stagnation point
y^+ dimensionless distance of the first point off the blade surface
z z-coordinate along the span
z^+ dimensionless distance of the first point off the hub or off the shroud
β_1 relative flow angle at entry to the rotor
γ ratio of specific heats
Ω rotational speed of the blade
ρ density

Subscripts

c for coolant (average value)
ex value at exit of rotor
m maximum value
o stagnation value
rel value relative to the rotor
w at the blade surface

1. INTRODUCTION

In order to extend component life, the use of film cooling in the design of turbine airfoils has been widespread. To minimize the usage of coolant flow, designers need to have an accurate prediction of the component heat load and film cooling effectiveness. The harsh operational environment as well as the high rates of rotational speed have combined to slow the progress in the understanding of the blade surface heat load in the presence of film cooling. Many studies on film cooling have been confined to simple geometries, for example, two-dimensional flat and curved plates in steady, incompressible flow. An excellent survey of the work up to 1971 has been provided by

Presented at the International Gas Turbine and Aeroengine Congress & Exhibition
Birmingham, UK — June 10-13, 1996

Goldstein (1971). While several further studies in this field have been summarized by Garg and Gaugler (1993, 1994, 1995), some relevant ones are discussed here.

Three detailed experimental measurements of film cooling on rotating turbine blades are available in the open literature. These investigations were presented by Dring et al. (1980), Abhari (1991), and Takeishi et al. (1991). All three studies concluded that film cooling on the suction surface provides good surface protection, while on the pressure surface the results are mixed. The measurement database of Abhari (1991), being the only experimental measurement of surface heat transfer for a film cooled rotating transonic turbine blade, provides the experimental results for the present numerical study. Abhari and Epstein (1994) also showed that the unsteady rotor-stator interaction results in the pulsation of the film cooling out of the holes. This coolant pulsation was later shown by Abhari (1996) to result in a considerable reduction on the pressure surface film effectiveness while the suction surface was relatively unaffected.

In the past few years, advances in the numerical techniques have resulted in the development of a number of different approaches specifically related to the study of film cooling. Many different approaches to the prediction of film cooling performance have been developed over the years. By far the most prevalent approach has been to model or correlate the penetration, spreading and entrainment of the main flow by the coolant jets from the discrete holes. These interaction models have been incorporated into boundary layer codes (Crawford et al. 1980; Schönung and Rodi, 1987; Tafti and Yavuzkurt, 1990) or into two dimensional Navier Stokes CFD code (Abhari, 1996). In another approach, Garg and Gaugler (1993, 1994, 1995) used a three dimensional CFD code with surface injection to model the film cooling performance around the C3X vane, and the VKI and ACE rotor cascades. In this approach, similar to the present technique, the film holes are modeled by adding, as a boundary condition, the appropriate amount of mass, momentum, and energy flux distribution at the discrete location of the film holes. They compared the predictions to the experimental measurements on these cascades and found a fairly good agreement. The computational results clearly illustrated the three dimensionality of the flow in the near hole region. Choi (1993) also used a three dimensional CFD code to predict the flow and the surface heat transfer around a section of the ACE turbine blade. The computational grid was extended into the film holes to model the elliptic nature of the flow at the film hole exit plane. In order to minimize the size of the computational grid and the associated computational resource requirements, Choi only modeled a section of the blade which in the span-wise direction covered one half of a film hole pitch with span-wise periodic boundary conditions. Such a reduction in computational span is possible, however, for a linear cascade only, and was also used by Garg and Gaugler (1993, 1994, 1995). For a rotating blade, the entire span needs to be discretized in order to model correctly the rotational body forces. Choi obtained a good comparison between the prediction of the surface heat flux with film cooling and the measured data on a two dimensional cascade.

The goal of the present study is to provide a better insight into the interaction of film coolant flow and the external flow in a transonic turbine including the influence of rotation and three dimensionality. The present approach is to numerically model the exact experimental conditions of an extensive measurement study by Abhari (1991) using the ACE turbine blade. The experimental results without film cooling were used to further validate the predictive capability of the CFD code. Then a number of operating conditions with film cooling were simulated and the predicted results compared to the experimental data. These comparisons combined with observations from the three dimensional numerical flow visualization are used to validate the present numerical approach for the film cooling of rotor blades and make observations on the influence of three dimensional external flow on the film coolant flow.

2. ANALYSIS

The three-dimensional Navier-Stokes code of Arnone et al. (1992) for the analysis of turbomachinery flows was modified by Garg and Gaugler (1994) to include film cooling effects. Briefly, the code is an explicit, multigrid, cell-centered, finite volume code with an algebraic turbulence model. The governing equations solved are the conservative form of the Reynolds averaged Navier-Stokes equations in a curvilinear coordinate system in terms of the absolute velocity and specific total energy. The perfect gas law is used as the equation of state. Variation of viscosity with temperature is assumed to follow Sutherland's law (Schlichting, 1979). The four-stage Runge-Kutta scheme developed by Jameson et al. (1981) is used to advance the flow solution in time from an initial guess to the steady state. To accelerate convergence the code employs the Full Approximation Storage (FAS) multigrid method originally devised by Brandt (1979) and Jameson (1983). Variable coefficient implicit smoothing of the residuals is performed to improve further the rate of convergence. A three-dimensional extension of eigenvalue scaling of the artificial dissipation terms, first devised by Martinelli (1987), was adopted to prevent odd-even decoupling and to capture shocks. Further details of the numerical scheme and implementation of the boundary conditions are given in Arnone (1993) and Arnone et al. (1992).

The effects of film cooling have been incorporated into the code in the form of appropriate boundary conditions at the hole locations on the blade surface. Each hole exit is represented by several control volumes having a total area equal to the area of the hole exit, and passing the same coolant mass flow, with the discharge coefficient for the hole having been taken into account. Different velocity and temperature profiles for the injected gas can be specified at the hole exit. For the cases reported here, uniform profiles for the coolant velocity (relative to the blade) and temperature distribution at the hole exit were specified. Also, one case was run with a polynomial distribution (Garg and Gaugler, 1995) of coolant velocity and temperature at the exit of the double-row of holes on the pressure surface in order to ascertain if that would bring the predicted and experimental results closer on the pressure surface.

The experimental values for the blade temperature were known at only 25 points on the blade surface, while the computational grid had over 38,000 grid points on the blade surface. Thus, in the absence of a complete surface temperature map, the blade surface was considered isothermal. The largest experimental variations in the blade surface temperature relative to the mean were as much as 10% from the mean for the fully film-cooled test cases. The hub and shroud surfaces were also considered isothermal and assumed to be at the same temperature as the blade. Based upon an estimate obtained from a streamline curvature prediction, the boundary layer thickness on the hub and shroud was taken to be 10% and 15% of span for the incoming flow to the rotor. The vena contracta of each hole was accounted for by reducing the actual hole exit area by the values of the estimated discharge coefficients, C_D, reported in the Table 1. The algebraic mixing length turbulence model of Baldwin and Lomax (1978) was used. This model was designed for the prediction of wall bounded turbulent shear layers, and may not be appropriate for flows with massive separations or large vortical structures. Thus, this model is likely to be invalid in a number of turbomachinery applications, but for turbine blades, the boundary layers generally experience a favorable pressure gradient whereby this model is more likely to be valid. It has been used satisfactorily by Boyle and Giel (1992), Ameri and Arnone (1994a, b), and Boyle and Ameri (1994) for heat transfer calculations on rotating turbine blades without film cooling, by Hall et al. (1994), and Garg and Gaugler (1994, 1995) on planar cascades with film cooling. In fact, Ameri and Arnone (1994b) compared the Baldwin-Lomax model and Coakley's q-ω model (Coakley, 1983) against the experimental data of Graziani et al. (1980), and found that the algebraic model was able to produce many of the flow features better than the two-equation model. They further state that this conclusion is strengthened when one takes into account the relative economy of computations with the algebraic model. It is known (Amer et al., 1992) that two-equation models are also not satisfactory in the presence of film cooling. Perhaps the multiple-time-scale turbulence model of Kim and Benson (1992) may be more appropriate. However, use of this model is computationally very expensive since it involves solving four more partial differential equations in addition to the five at present, all coupled.

3. ACE ROTOR AND EXPERIMENTAL DETAILS

The Rolls-Royce ACE high pressure transonic turbine model was the test object on which film cooling data were taken in the short duration (0.3 second measurement time), blowdown, rotating turbine rig facility at M.I.T. by Abhari (1991). In this facility, it is possible to simulate full engine scale Reynolds number, Mach number, Prandtl number, gas to wall and coolant to mainstream temperature ratios, specific heat ratios, and flow geometry while operating under benign operating conditions. The turbulent intensity at the nozzle guide vane inlet was less than 1%. A mixture of argon and freon-12 was used for the main flow while a mixture of argon and freon-14 was used as the coolant in order to prevent condensation at the low temperatures and high pressures of the coolant supply system. Values of the gas constant and specific heat ratios for the mainstream and coolant flows are given in Table 1.

The ACE turbine geometry and cooling arrangement are shown schematically in Fig. 1. This turbine had a 551.2 mm rotor diameter with 36 nozzle guide vanes (NGV's) and 61 rotor blades. The rotor blades had an axial chord of 26.1 mm, and five film cooling rows containing 93 holes. For the cooled rotor tests, thin walled NGV's were used with slot injection near the pressure surface trailing edge sized to pass the flow of a fully cooled NGV. Three instrumented and six other solid aluminum rotor blades were drilled out for two radially positioned coolant supply plenums; the other 52 rotor blades were of steel shell construction. The coolant film hole internal diameter was 0.5 mm for all holes. All rows had circular exit areas except for the first row (SS1) on the suction surface which was D-shaped. The cooling configuration consisted of: a) one 30° single row (SS1) of 18 D-shaped holes (fanned at 25° half angle in the spanwise direction with an exit width of 1.25 mm) at about 20% surface length on the suction surface, b) one 30° single row (SS2) of 20 round holes at about 70% surface length on the suction surface, c) one 60° single row (PS1) of 18 holes at about 25% surface length on the pressure surface, and d) one 30° double row of 19 (PS21) and 18 (PS22) staggered holes, with a chordwise spacing of 2 mm, at about 50% surface length on the pressure surface. All holes were drilled at 90° from the radial direction. More details in terms of estimated discharge coefficient for the holes are available in Table 1. Figure 2 shows a small portion of the unfolded part of the blade containing the holes. The ordinate in Fig. 2 denotes the distance along the blade surface in the spanwise direction, while the abscissa denotes the distance, measured from the leading edge, along the blade surface in the streamwise direction, both normalized by the hole diameter, d. The shape and orientation of the hole openings in Fig. 2 is a direct consequence of the angles the holes make with the spanwise or streamwise direction.

The heat flux from the free-stream to the blade was measured with thin film heat flux gauges distributed about the blade profile. These transducers are 25 μm thick with a rectangular sensing area (1.0 × 1.3 mm), oriented such that the longest dimension is in the chordwise direction. The coolant hole and heat flux gauge locations are shown in Fig. 3. The top chordwise row will be referred to as the tip location, the middle as mid-span, and the bottom as the hub gauges. Note that none of the three rows of gauges is at a fixed radial location. Unfortunately, several of the gauges failed over the course of the testing, especially on the pressure surface. Thus, not all measurement locations yielded data at all test conditions. High frequency response pressure transducers and thermocouples were installed in the NGV's and rotor blades to monitor the conditions in the coolant hole supply plenums. All worked well except for the rotor thermocouples which were unreliable. Facility measurements included inlet total temperature and pressure, outlet total pressure, wall static pressures, and rotor speed. More details are available in Abhari (1991).

4. COMPUTATIONAL DETAILS

Since the cylindrical hole diameter is 0.5 mm, the grid size has to be varied along the blade chord. For computational accuracy, the ratio of two adjacent grid sizes in any direction was kept within 0.76 to 1.3. A periodic C-grid with over 2,278,000 grid points was used. The grid used was 225x45x225 where the first number represents the number of grid points along the main flow direction, the second in the blade-to-blade direction, and the third in the span direction. This grid was arrived at following numerical experimentation with a coarser grid 133×41×113, and discussions with co-workers. Normal to the blade surface is the dense viscous grid, with $y^+ < 1.0$ for the first point off the blade surface, following Boyle and Giel (1992), and Hall et al. (1994). Normal to the hub and shroud also is a dense grid, with $z^+ < 2.5$ for the first point off the hub or off the shroud. Also, the tip clearance region was taken to be 1% of the blade span (static measurement) with 20 grid points within it. The tip clearance region is handled by imposing periodicity conditions across the airfoil. Computations were run on the 16-processor C-90 supercomputer at NASA Ames Research Center. The code requires about 130 million words (Mw) of storage and takes about 45 s per iteration (full-multigrid) on the C-90 machine. For a given grid the first isothermal blade case requires about 1000 iterations to converge, while subsequent cases (corresponding to different values of the parameters) for the same grid require about 400 iterations starting with the solution for the previous case.

5. RESULTS AND DISCUSSION

The present numerical results were obtained by simulating the exact experimental conditions of the MIT experiment given in Table 1 for the cases compared. The blowing parameter, B_p, and the coolant temperature, T_c/T_o, at the hole exits were estimated from the static pressure distribution on an uncooled blade (found by executing the present code in the uncooled mode), and the relative total pressure and temperature measured in the coolant plenums, with coolant Mach number, relative to the rotor, restricted to unity at the hole-exit. All holes in the second row (SS2) and most holes in the first row (SS1), especially those near the hub, on the suction surface were choked. Besides the three film-cooled cases, Run # 71, 72 and 73, an uncooled case, Run # 61, was also selected for comparison, as detailed in Table 1. While case # 71 represents near design-condition operation, test case # 73 represents a lower pressure ratio and speed, and case # 72 has a positive incidence angle. Figure 4 shows the computed relative flow angle at the rotor inlet; the symbols on this figure represent the predicted values from a through-flow streamline curvature calculation, while the curves belong to the 3-D calculation based on the present code. The effect of boundary layers on the hub and shroud is clearly reflected in Fig. 4.

Figure 5 compares the computed Nusselt number on the blade surface near the mid-span with the experimental data for the non-film-cooled case # 61. The Nusselt number is based on the rotor axial chord, the relative total temperature at entry to the rotor, the blade temperature, and the gas thermal conductivity at the blade temperature. The abscissa is the fractional wetted pressure and suction surface of the blade. The experimental data is shown with error bars. Comparison at the leading edge and all along the suction surface is very good (within 10%) but on the pressure surface the prediction is approximately 30% lower than the data at all locations. This comparison suggests that, in the absence of film cooling, the present approach is correctly simulating the driving mechanisms for heat transfer on the suction surface. Reasons for the under-prediction on the pressure surface are cited later.

Figure 6 compares the computed Nusselt number on the blade surface near the hub, mid-span and tip with the experimental data for the film-cooled baseline case # 71. Presence of negative values of Nu at some locations simply implies that the direction of heat transfer is reversed at these locations due to specification of the isothermal wall boundary condition and coolant temperature. The comparison is very good at the leading edge, generally good on the suction surface but fairly poor downstream of PS1 on the pressure surface near the hub. It is interesting to note that near the hub section, where the best experimental data coverage is available, the suction surface heat transfer is very well predicted both in terms of the level and the distribution of surface heat flux. On the pressure surface, however, the prediction completely underpredicts the heat transfer. The large radial migration of the coolant film on the pressure surface, as shown by Dring et al. (1980) on a low speed rig, was not observed in the present calculations.

In Figures 7 and 8, similar comparisons of numerical prediction of Nusselt number with the experimental data for film-cooled cases # 72 and # 73 are shown, respectively. There are a number of possible reasons for the poor comparison with the experimental data on the pressure surface. There is a strong evidence (Abhari, 1996) that the periodic flow unsteadiness resulting from the stator-rotor interaction fundamentally changes the coolant jet/main flow interaction on the pressure surface, while the suction surface is relatively unaffected. The present calculation being steady-state does not model this unsteadiness. In the experimental tests, however, the rotor blades interact with the shock, wakes and the potential field of the upstream nozzle guide vanes resulting in a highly unsteady flow structure (Abhari et al. 1992). This is true whether the blade is cooled or uncooled. Another possible cause of this discrepancy for the cooled rotor can be the result of uncertainty in the values of the blowing parameter, coolant temperature, and the relative flow angle at inlet to the rotor which were all estimated by matching the values from a through-flow streamline curvature calculation, in the absence of experimental measurements, with the present code. Also, the gas constant and specific heat ratios for the mainstream and coolant flow are different in the experiment owing to the use of different gas mixtures but the code assumes the same gas for both the main and coolant flows. Moreover, values of the discharge coefficients for the film-cooling holes were estimated, not measured. Finally, it is possible that the turbulent mixing on the low Mach number pressure surface is under-predicted by the turbulence model. While the results in Figs. 6-8 are based on a uniform coolant velocity and temperature distribution at the hole exits, specifying a polynomial distribution, like that in Garg and Gaugler (1995), at the exit of the double-row of holes on the pressure surface does not improve the comparison by more than 5%.

In Figure 9, the present 3-D computation of Nusselt number is compared with the predictions from a 2-D Navier-Stokes code with a film injection model (Abhari, 1996) and experimental data for cases # 71 and # 72 near mid-span. The 2-D calculation seems to give a higher level of the Nusselt number values compared to the 3-D code almost everywhere around the airfoil. The predictions from the present 3-D code provide a much better comparison to the experimental data for the leading edge heat transfer than the 2-D prediction reported by Abhari (1996). Figure 10 shows Nusselt number contours at intervals of 200 over the entire blade surface for the one uncooled and three cooled cases. Due to no film cooling over the leading edge portion, this part of the blade has a high Nusselt number, being exposed to the hot stream for all the four cases. Downstream of the first and subsequent rows of cooling holes on both the pressure and suction surfaces, the effect of film cooling is clearly evident as streaks of lower heat load and generally lower Nusselt number values as compared to the uncooled case. For the off-design case # 72, the blade suction surface upstream of the second row of holes has higher Nusselt number values than the other cooled cases. It also has higher Nu values on the leading edge portion. On the other hand, case # 73 has lower Nu values than all the other cases over the entire blade surface, and is thus the best-cooled case studied. It may also be observed that the Nusselt number is fairly high in the thick boundary layers on the suction surface near both the hub and the tip. From this figure, we observe that the Nusselt number is a strong function of the streamwise as well as the spanwise location, especially in the vicinity of film-cooling holes.

6. CONCLUSIONS

As far as the authors are aware of, the present study provides the first comparison of surface heat transfer between a fully three dimensional CFD code with film injection and the experimental data obtained on a transonic rotating rotor blade with film cooling. The present approach was shown to provide a reasonably good prediction of the heat transfer at the leading edge and on the suction surface of a film cooled rotor blade when compared to the experimental data, validating the code under blade rotation. On the pressure surface, the code under-predicted the surface heat transfer. Reasons for differences on the pressure surface are cited; most plausible one seems to be the presence of unsteady effects due to stator-rotor interaction in the experiments which are neglected in the present computations. It is found that the Nusselt number on the blade surface is highly three-dimensional in the vicinity of holes but tends to become two-dimensional far downstream.

ACKNOWLEDGEMENTS

The first author wishes to thank Dr. Raymond Gaugler, Chief, Turbomachinery Flow Physics Branch, and Mr. Peter Batterton, Manager, Advanced Subsonic Technology Program at the NASA Lewis Research Center for their support of this work. The experimental results reported in this work were supported by the Wright Laboratories, USAF, Dr. C. McArthur, program monitor, and Rolls-Royce Inc., Dr. R.J.G. Norton, technical monitor.

REFERENCES

Abhari, R.S., 1991, "An Experimental Study of the Unsteady Heat Transfer Process in a Film Cooled Fully Scaled Transonic Turbine Stage," Ph.D. Thesis, Massachusetts Institute of Technology.

Abhari, R.S., 1996, "Impact of Rotor-Stator Interaction on Turbine Blade Film Cooling," *J. Turbomachinery*, to appear.

Abhari, R.S. and Epstein, A.H., 1994, "An Experimental Study of Film Cooling in a Rotating Transonic Turbine," *J. Turbomachinery*, Vol. 116, pp. 63-70.

Abhari, R.S., Guenette, G.R., Epstein, A.H., and Giles, M.B., 1992, "Comparison of Time-Resolved Measurements and Numerical Calculations," *J. Turbomachinery*, Vol. 114, pp. 818-827.

Amer, A.A., Jubran, B.A. and Hamdan, M.A., 1992, "Comparison of Different Two-Equation Turbulence Models for Prediction of Film Cooling from Two Rows of Holes," *Numer. Heat Transfer*, Vol. 21, Part A, pp. 143-162.

Ameri, A.A., 1994, "Transition Modeling Effects on Turbine Rotor Blade Heat Transfer Predictions," NASA CP 3282, Vol. II, pp. 20-28.

Ameri, A.A. and Arnone, A., 1994a, "Transition Modeling Effects on Turbine Rotor Blade Heat Transfer Predictions," ASME Paper 94-GT-22.

Ameri, A.A. and Arnone, A., 1994b, "Prediction of Turbine Blade Passage Heat Transfer Using a Zero and a Two-Equation Turbulence Model," ASME Paper 94-GT-122.

Arnone, A., 1993, "Viscous Analysis of Three-Dimensional Rotor Flow Using a Multigrid Method," ASME Paper 93-GT-19.

Arnone, A., Liou, M.-S. and Povinelli, L.A., 1992, "Navier-Stokes Solution of Transonic Cascade Flows Using Non-Periodic C-type Grids," *J. Propul. & Power*, Vol. 8, pp. 410-417.

Baldwin, B.S. and Lomax, H., 1978, "Thin-Layer Approximation and Algebraic Model for Separated Turbulent Flows," AIAA Paper 78-257.

Boyle, R.J. and Ameri, A.A., 1994, "Grid Orthogonality Effects on Predicted Turbine Midspan Heat Transfer and Performance," ASME Paper 94-GT-123.

Boyle, R.J. and Giel, P., 1992, "Three-Dimensional Navier Stokes Heat Transfer Predictions for Turbine Blade Rows," AIAA Paper 92-3068.

Brandt, A., 1979, "Multi-Level Adaptive Computations in Fluid Dynamics," AIAA Paper 79-1455.

Choi, D., 1993, "A Navier-Stokes Analysis of Film Cooling in a Turbine Blade," AIAA Paper 93-0158.

Coakley, T.J., 1983, "Turbulence Modeling Methods for the Compressible Navier-Stokes Equations," AIAA Paper 83-1693.

Crawford, M.E., Kays, W.M. and Moffat, R.J., 1980, "Full Coverage Film Cooling on Flat, Isothermal Surfaces: A Summary Report on Data and Predictions," NASA CR 3219.

Dring, R.P., Blair, M.F. and Joslyn, H.D., 1980, "An Experimental Investigation of Film Cooling on a Turbine Rotor Blade," *J. Eng. Power*, Vol. 102, pp. 81-87.

Garg, V.K. and Gaugler, R.E., 1993, "Heat-Transfer in Film-Cooled Turbine Blades," ASME Paper 93-GT-81.

Garg, V.K. and Gaugler, R.E., 1994, "Prediction of Film Cooling on Gas Turbine Airfoils," ASME Paper 94-GT-16.

Garg, V.K. and Gaugler, R.E., 1995, "Effect of Velocity and Temperature Distribution at the Hole Exit on Film Cooling of Turbine Blades," ASME Paper 95-GT-2. (Also to appear in *J. Turbomachinery*).

Goldstein, R.J., 1971, "Film Cooling," *Advances in Heat Transfer*, Vol. 7, pp. 321-379.

Graziani, R.A., Blair, M.F., Taylor, J.R. and Mayle, R.E., 1980, "An Experimental Study of Endwall and Airfoil Surface Heat Transfer in a Large Scale Turbine Blade Cascade," *J. Eng. Power*, Vol. 102, pp. 257-267.

Haas, W., Rodi, W. and Schönung, B., 1991, "The Influence of Density Difference Between Hot and Coolant Gas on Film Cooling by a Row of Holes: Predictions and Experiments," ASME Paper 91-GT-255.

Hall, E.J., Topp, D.A. and Delaney, R.A., 1994, "Aerodynamic/Heat Transfer Analysis of Discrete Site Film-Cooled Turbine Airfoils," AIAA Paper 94-3070.

Jameson, A., 1983, "Transonic Flow Calculations," MAE Report 1651, MAE department, Princeton University.

Jameson, A., Schmidt, W. and Turkel, E., 1981, "Numerical Solutions of the Euler Equations by Finite Volume Methods Using Runge-Kutta Time-Stepping Schemes," AIAA Paper 81-1259.

Kim, S.-W. and Benson, T.J., 1992, "Calculation of a Circular Jet in Cross Flow with a Multiple-Time-Scale Turbulence Model," *Intl. J. Heat Mass Transfer*, Vol. 35, pp. 2357-2365.

Leylek, J.H. and Zerkle, R.D., 1994, "Discrete-Jet Film Cooling: A Comparison of Computational Results With Experiments," *J. Turbomachinery*, Vol. 116, pp. 358-368.

Martinelli, L., 1987, "Calculations of Viscous Flows With a Multigrid Method," Ph.D. Thesis, Princeton University.

Schlichting, H., 1979, *Boundary Layer Theory*, 7th Ed., McGraw-Hill, New York, p. 328.

Schönung, B. and Rodi, W., 1987, "Prediction of Film Cooling by a Row of Holes with a Two-Dimensional Boundary-Layer Procedure," *J. Turbomachinery*, Vol. 109, pp. 579-587.

Tafti, D.K. and Yavuzkurt, S., 1990, "Prediction of Heat Transfer Characteristics for Discrete Hole Film Cooling for Turbine Blade Applications," *J. Turbomachinery*, Vol. 112, pp. 504-511.

Takeishi, K., Aoki, S., Sato, T. and Tsukagoshi, K., 1991, "Film Cooling on a Gas Turbine Rotor Blade," ASME Paper 91-GT-291.

Table 1 Parameter Values

Main Flow Parameters: R = 125.1 J/kg-K

Case	p_o(kPa)	T_o (K)	p_{ex} (kPa)	Ω (rpm)	T_w (K)	γ
71	450.0	486.0	117.537	7087	321.3	1.246
72	460.0	490.0	128.683	5610	325.0	1.255
73	351.0	417.0	92.206	6330	310.0	1.276
61	458.0	500.0	93.219	7380	310.0	1.237

Coolant Flow Parameters: R_c = 158.5 J/kg-K

Case	γ_c	$T_{o,rel}$ (K)	$p_{o,rel}$ (kPa)		
			hub	mid-span	tip
71	1.406	222.5	241.761	255.238	262.229
72	1.405	224.5	258.683	268.410	275.503
73	1.406	222.9	194.645	204.373	212.276

Hole Characteristics: Hole diameter = 0.5 mm, spanwise pitch = 2 mm, spanwise angle = 90°

Hole-row	estimated discharge coefficient, C_D									stream-wise angle (deg)	hole-shape	# of holes
	Hub for case			Mid-span for case			Tip for case					
	71	72	73	71	72	73	71	72	73			
PS1	0.52	0.63	0.57	0.64	0.66	0.64	0.63	0.67	0.66	60	cylinder	18
PS21	0.50	0.63	0.62	0.62	0.64	0.64	0.60	0.65	0.65	30	cylinder	19
PS22	0.56	0.63	0.61	0.62	0.64	0.63	0.64	0.65	0.64	30	cylinder	18
SS1	0.52	0.37	0.52	0.59	0.45	0.56	0.62	0.56	0.61	30	D-shape	18
SS2	0.48	0.48	0.48	0.39	0.39	0.39	0.46	0.46	0.46	30	cylinder	20

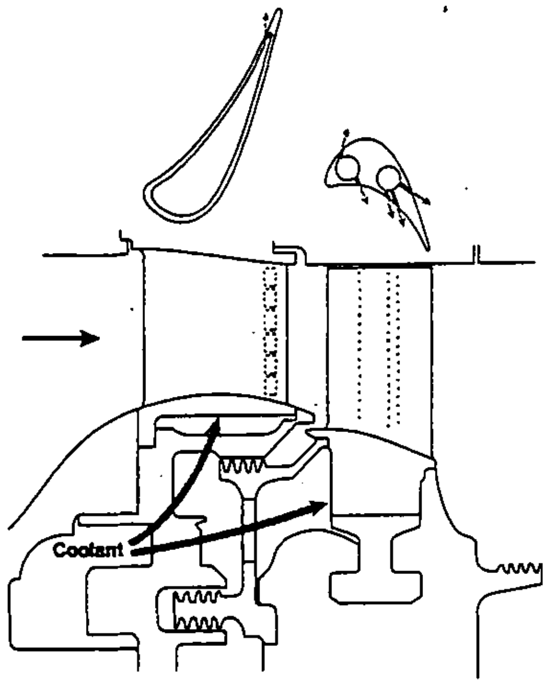

Fig. 1 ACE turbine geometry and cooling arrangement

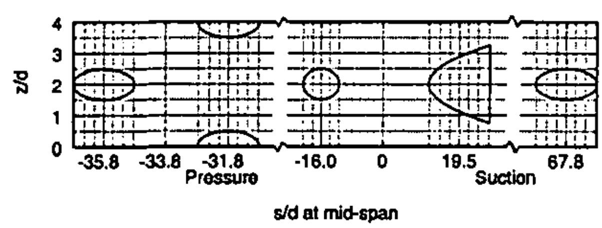

Fig. 2 Shape of film cooling holes at exit on the ACE rotor surface

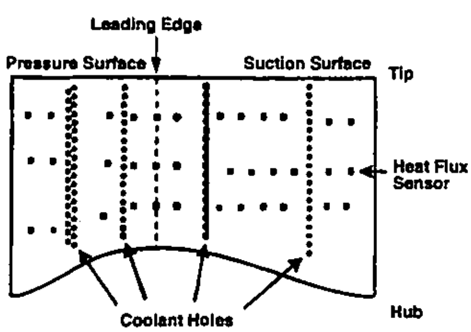

Fig. 3 Heat flux gauges and cooling hole locations on the projected blade surface with each of the three chordwise rows of gauges on a separate blade

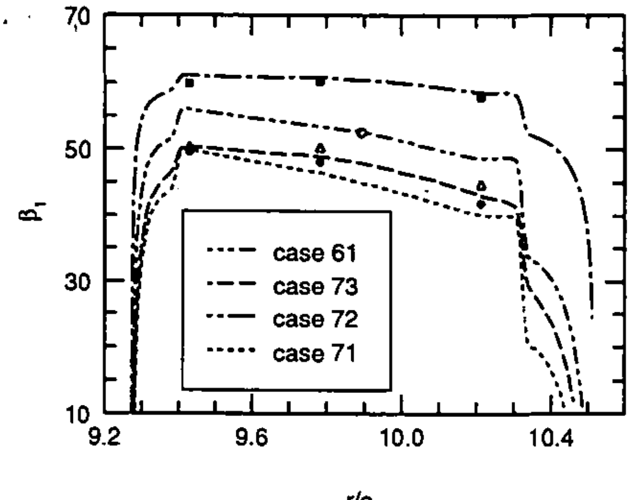

Fig. 4 Relative flow angle at rotor inlet as a function of spanwise location

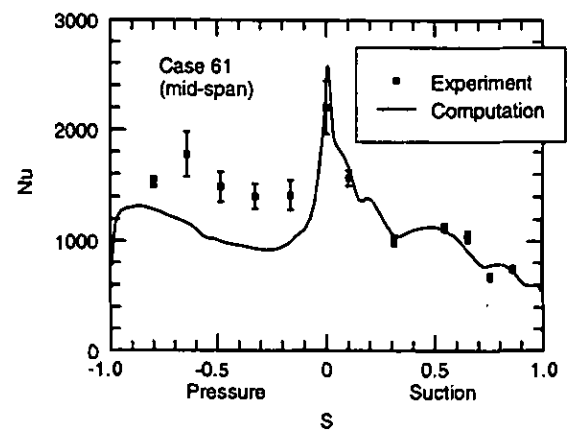

Fig. 5 Comparison of Nusselt number on the blade surface for uncooled case 61 near mid-span

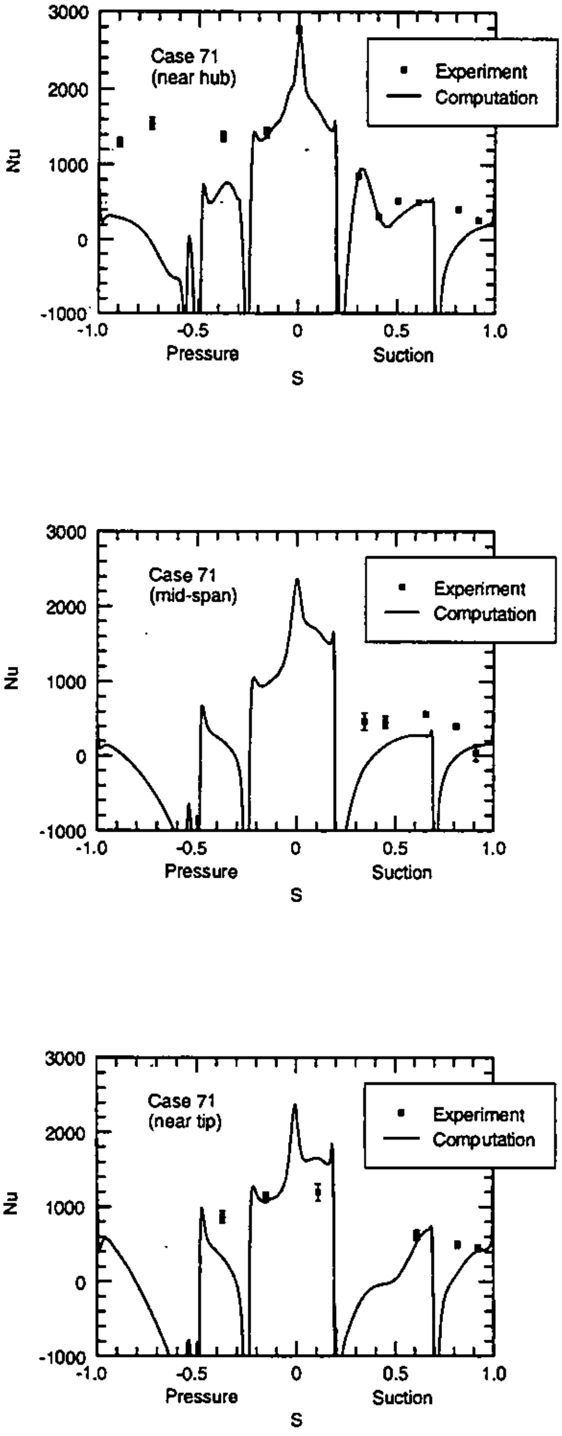

Fig. 6 Comparison of Nusselt number on the blade surface for case 71 near hub, mid-span and tip

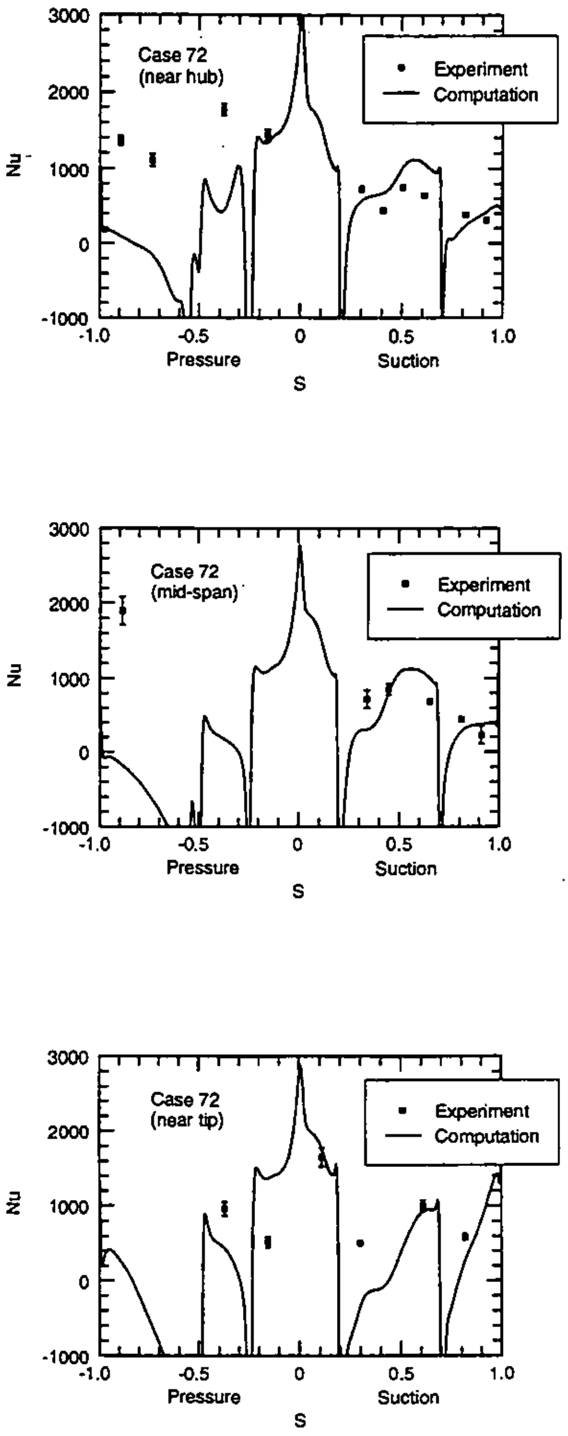

Fig. 7 Comparison of Nusselt number on the blade surface for case 72 near hub, mid-span and tip

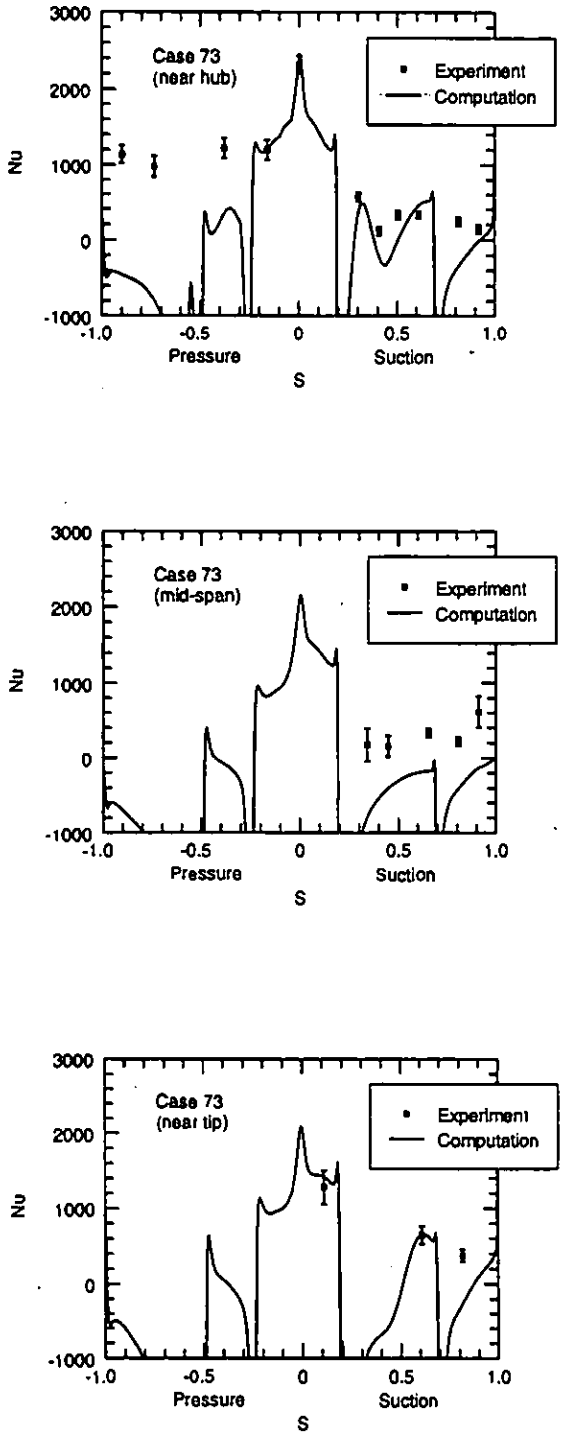

Fig. 8 Comparison of Nusselt number on the blade surface for case 73 near hub, mid-span and tip

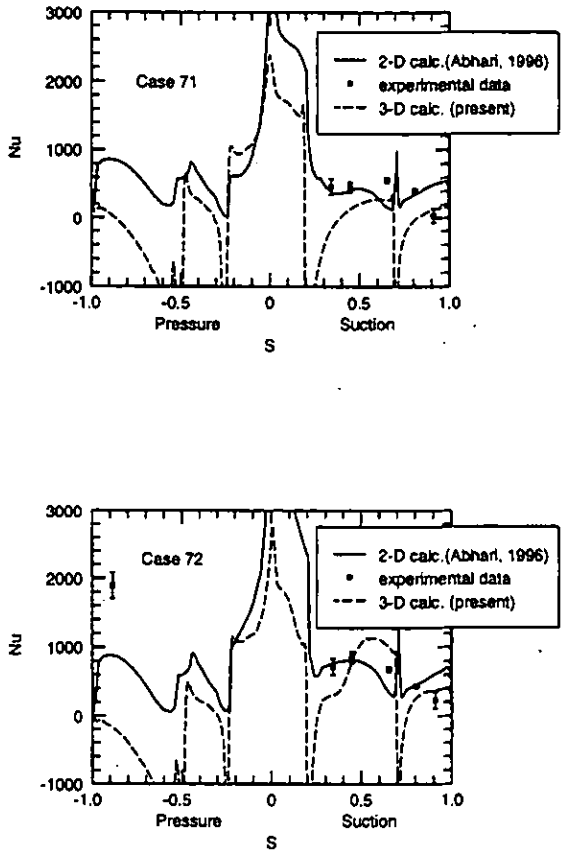

Fig. 9 Comparison of Nusselt number on the blade surface for cases 71 and 72 near mid-span

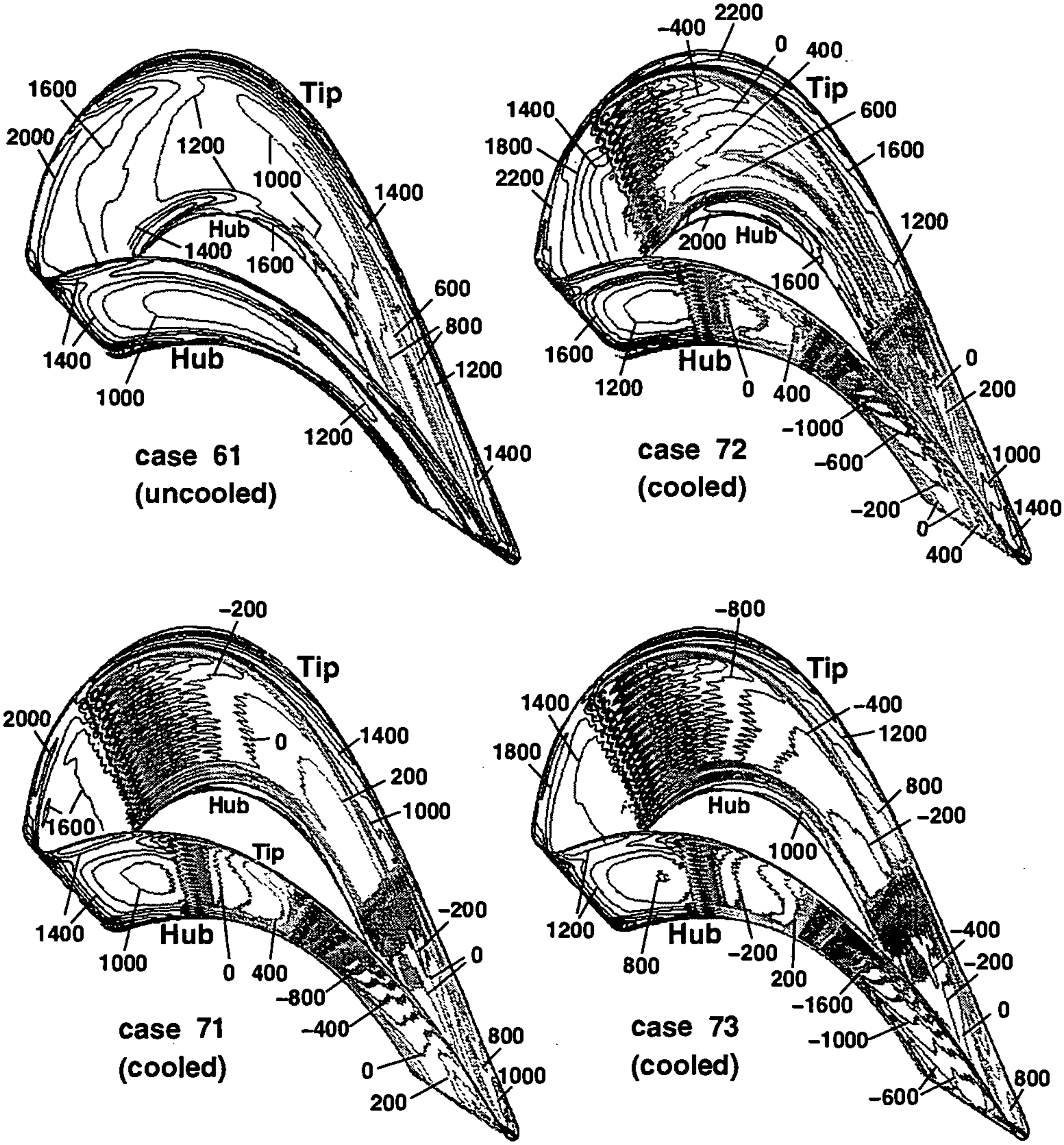

FIG. 10 NUSSELT NUMBER CONTOURS ON THE ACE ROTOR FOR VARIOUS CASES